

## On the stress induced InGaN/GaN quantum wells and quantum dots

Jun Chen<sup>1</sup>, Huaping P. Lei<sup>2</sup>, Pierre Ruterana<sup>2</sup>, Gerard Nouet<sup>2</sup>, Amina Belkadi<sup>3</sup>, and Paweł Dłużewski<sup>3</sup>

<sup>1</sup> Laboratoire de Recherche sur les Propriétés des Matériaux Nouveaux, Institut Universitaire de Technologie d'Alençon, 61250 Damigny, France,

<sup>2</sup> Structure des Interfaces et Fonctionnalité des Couches Minces (SIFCOM), UMR CNRS 6176, ENSICAEN, 6 Boulevard du Maréchal Juin 14050 Caen, France,

<sup>3</sup> Interdisciplinary Center of Materials Modeling, Institute of Fundamental Technological Research PAS, Świątokrzyska 21, 00-049 Warsaw, Poland.

e-mail: jun.chen@unicaen.fr

The lattice distortion field is extracted by computer image processing with the HRTEM image of GaN structure. Using a 3D nonlinear finite element method, the segregation of Indium atoms in a quantum dot is interpreted by residual stresses from a threading dislocation. The formation of Indium clusters is considered in terms of molecular dynamics and finite element method. Using the Stillinger-Weber potential and molecular dynamics, a systematic analysis of the energy of these In-rich clusters in a quantum well (QW) was carried out. The quantum wells, 4 atomic monolayers width, contain 30% at Indium and are built between two GaN crystals. A comparison of their relative stability with the random alloys of the same composition was done with different sizes of the clusters. It was shown that an In random distribution in the QW is favoured, but for specific conditions the energy difference is low, and the formation of the In-rich clusters could be possible.

*Keywords: molecular dynamics, nonlinear finite element method, stress induced diffusion*

### 1. Introduction

III-V nitride semiconductors (GaN, InN) are now involved in a large domain of optoelectronic applications: blue light emitting diodes and lasers due to their direct band gap in the range 0.7-6.2eV. The first blue laser was carried out with an  $\text{In}_x\text{Ga}_{1-x}\text{N}$  quantum well structure. In these ternary alloys, segregation, phase separation or ordering can occur due to the large difference in bond lengths of the two nitrides, GaN and InN. The formation of Indium rich clusters in the epitaxial layers of InGaN quantum well was observed at the atomic scale by means of High Resolution Transmission Electron Microscopy (HRTEM). These Indium clusters should be the key word to understand the mechanisms of light emission in GaN/ $\text{In}_x\text{Ga}_{1-x}\text{N}$ /GaN quantum wells. However, the origin of these In-rich clusters is still indeterminate: due to a phase separation or just an effect of the electron beam damages in TEM. In the same way, residual stresses induced by defects as threading dislocations can affect the diffusion process of In, Ga species controlling the segregation; this process is simulated step by step by using a 3D nonlinear FE method in  $\text{In}_x\text{Ga}_{1-x}\text{N}$  layer deposited on GaN. From the thermodynamical point of view, this process is governed by the driving force induced by the gradient of residual stresses operating in an anisotropic nonlinear elastic structure. The source of stresses we consider is the set of threading dislocations examined in a HRTEM plane view of GaN layer deposited on sapphire.

### 2. Finite element analysis

#### 2.1. Continuum thermodynamics

Consider an interdiffusion process coupled with the mass transport in the wurtzite type  $\text{In}_x\text{Ga}_{1-x}\text{N}$  crystal lattice. Let the molar density of the energy be governed by the following constitutive equation

$$\psi = \frac{1}{2\hat{c}}(\hat{\boldsymbol{\epsilon}} - \hat{\boldsymbol{\epsilon}}_{\text{ch}}) : \hat{\boldsymbol{c}} : (\hat{\boldsymbol{\epsilon}} - \hat{\boldsymbol{\epsilon}}_{\text{ch}}) + \psi_{\text{ch}}, \quad (1)$$

where  $\hat{\boldsymbol{\epsilon}}$  is the strain of crystal lattice,  $\hat{c}$  is the total molar concentration referred to the perfect (undeformed) GaN lattice,  $\hat{\boldsymbol{c}}$  is the elastic stiffness tensor. The chemical strain is governed by the Vegard law

$$\hat{\boldsymbol{\epsilon}}_{\text{ch}} = \hat{\mathbf{a}}_{\text{InN}} x + \hat{\mathbf{a}}_{\text{GaN}} (1 - x), \quad (2)$$

where  $\hat{\mathbf{a}}_{\text{InN}}$  and  $\hat{\mathbf{a}}_{\text{GaN}}$  are tensors of the respective Vegard coefficients. A pure chemical part of energy  $\psi_{\text{ch}}$  is independent of strain and depends only on molar fraction of Indium  $x$ . In our case the elastic strain is identified with  $\hat{\boldsymbol{\epsilon}}_{\text{e}} = \hat{\boldsymbol{\epsilon}} - \hat{\boldsymbol{\epsilon}}_{\text{ch}}$ , cf. [1, 2, 3]. It can be shown that the substitution of (1) into the energy balance equation gives the following formula for the driving force governing diffusion

$$\hat{\mathbf{f}} = \nu(\hat{\mathbf{a}}_{\text{InN}} - \hat{\mathbf{a}}_{\text{GaN}}) : \hat{\boldsymbol{c}} : \widehat{\text{grad}} \hat{\boldsymbol{\epsilon}} - [a_{\text{ch}} + \nu(\hat{\mathbf{a}}_{\text{InN}} - \hat{\mathbf{a}}_{\text{GaN}}) : \hat{\boldsymbol{c}} : (\hat{\mathbf{a}}_{\text{InN}} - \hat{\mathbf{a}}_{\text{GaN}})] \widehat{\text{grad}} x, \quad (3)$$

where the colon denotes the double scalar product,  $\widehat{\text{grad}}$  means the gradient related to distances in a perfect (undeformed, stress

free) crystal lattice,  $a_{\text{ch}} = \frac{\partial^2 \psi_{\text{ch}}}{\partial x^2}$ , and  $\nu$  is a factor saying which part of the driving force is used for interdiffusion and mass transport, respectively. In our case the deformation of crystal lattice is considered in terms of so-called finite strains. We assume that the so-called total deformation gradient,  $\mathbf{F}$ , is decomposed multiplicatively into thermodynamically reversible deformation  $\mathbf{F}_{\text{e}}$  and irreversible deformation tensor  $\mathbf{F}_{\text{pl}}$ ,  $\mathbf{F} = \mathbf{F}_{\text{e}}\mathbf{F}_{\text{pl}}$ . For example, the plastic deformation rate tensor is defined as  $\hat{\mathbf{d}}_{\text{pl}} \stackrel{\text{df}}{=} \dot{\mathbf{F}}_{\text{pl}}\mathbf{F}_{\text{pl}}$ , where  $\dot{\mathbf{F}}_{\text{pl}}$  denotes the material derivative of  $\mathbf{F}_{\text{pl}}$ .

In our case the elastic strain is defined as  $\hat{\boldsymbol{\epsilon}}_{\text{e}} \stackrel{\text{df}}{=} \frac{1}{2} \ln(\mathbf{F}_{\text{e}}^T \mathbf{F}_{\text{e}})$ . More details on the thermodynamic approach used here is given in [3, 11]. According to the thermodynamic limitations we can assume the following constitutive equation for the diffusion velocity and inelastic strain rate resulting from the drugging of ma-

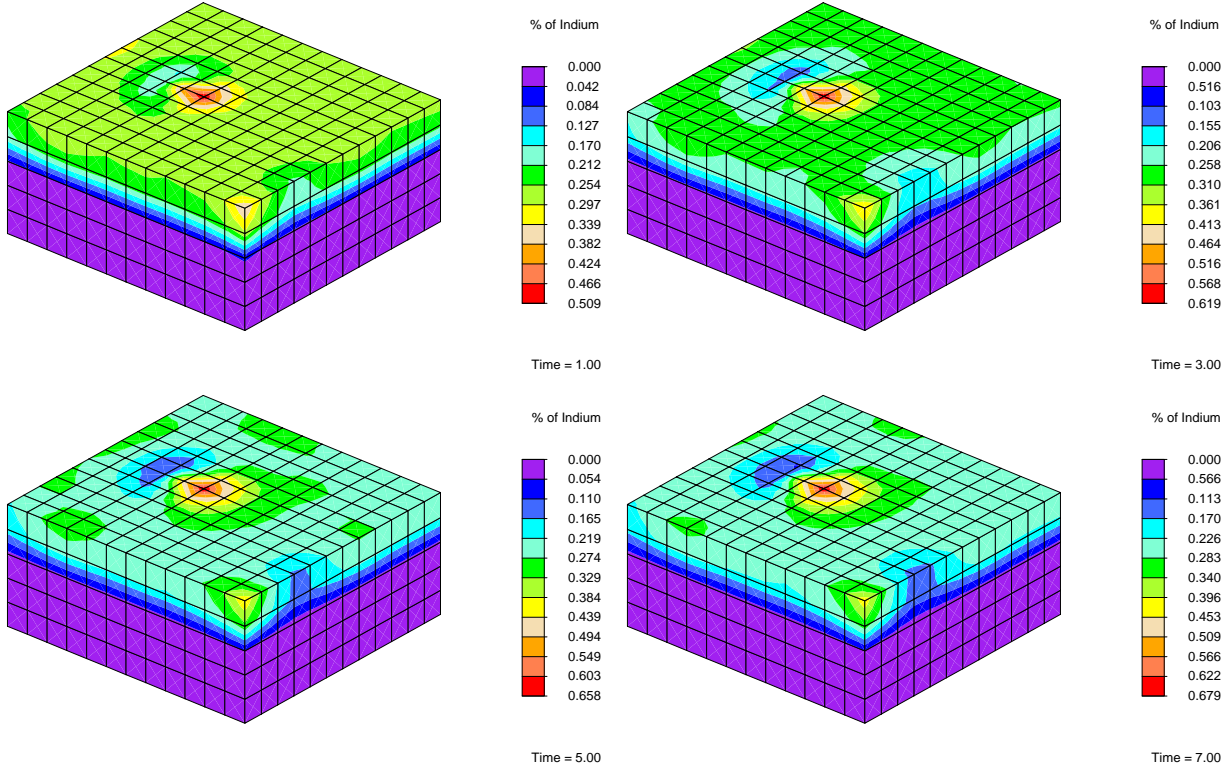


Figure 1: Subsequent time frames illustrating Indium concentrations around threading edge dislocation.

terial with interdiffusion

$$\widehat{\mathbf{v}}_d = \widehat{\mathbf{B}}\widehat{\mathbf{f}}, \quad (4)$$

$$\widehat{\mathbf{d}}_{pl} = -(1 - \nu)\widehat{\text{div}} [(\widehat{\mathbf{a}}_{In} - \widehat{\mathbf{a}}_{Ga}) \otimes \widehat{\mathbf{J}}], \quad (5)$$

where  $\widehat{\mathbf{J}} = \widehat{c}x\widehat{\mathbf{v}}_d$  and  $\widehat{\mathbf{B}}$  is a second-order positively defined tensor of diffusivity coefficients, see [3, 11].

## 2.2. FE simulation

Our FEM algorithm is based on integration of two balance equations

$$\text{div } \boldsymbol{\sigma} = \mathbf{0}, \quad (6)$$

$$c\dot{x} + \text{div}(cx\mathbf{v}_d) = 0, \quad (7)$$

where  $\mathbf{v}_d = \mathbf{F}_e\widehat{\mathbf{v}}_d$  and  $c = \widehat{c}\det \mathbf{F}_e^{-1}$ . The Cauchy stress depends on the gradient of displacement and on the Indium fraction,  $\boldsymbol{\sigma} = \boldsymbol{\sigma}(\nabla \mathbf{u}, x)$ . In terms of FEM the diffusion velocity is dependent on the first and second order gradients of displacement field and on the chemical fraction and its first gradient,  $\mathbf{v} = \mathbf{v}(\nabla \mathbf{u}, \nabla^2 \mathbf{u}, x, \nabla x)$ .

We used 27-node brick finite elements in which the shape function for displacements is spanned on all 27 nodes and based on the second-order Lagrangian polynomials, while for Indium fraction we used the first order Lagrangian polynomials spanned only on 8 corner nodes (multilinear shape function). In our FE simulation we have normalized the time of the process to obtain a final stress equilibrium of Indium concentrations in 10 time units. To this aim the following diffusivity coefficients were assumed in SI: for the 3D finite elements situated on InGaN surface  $B = 10^{-28}$  and for the GaN bulk elements  $B = 10^{-38}$ , where  $\widehat{\mathbf{B}} = \begin{bmatrix} B & & \\ & B & \\ & & B \end{bmatrix}$ . The time step was  $\Delta t = 0.1$ . In our simulations we have assumed  $\psi_{ch} = 0$  and  $\nu = 1$ . All other parameters were

assumed to be the same as those in our previous FE calculations, see [4]. The results are presented in Fig. 1. The FE results can be rescaled to any other (real) time scale of diffusion process by rescaling the mentioned diffusivity coefficients.

## 3. Molecular Dynamics

### 3.1. Stillinger-Weber empirical potentials for InGaN alloys

We used a modified Stillinger-Weber (SW) potential to undertake our atomistic calculation for the InGaN quantum well. This empirical potentials consider the two- and three-body interactions and are suitable to describe the total energy of the tetrahedral semiconductors

$$\Phi(1, \dots, N) = \sum_{\substack{i,j \\ (i < j)}} \phi_2(i, j) + \sum_{\substack{i,j,k \\ (i < j < k)}} \phi_3(i, j, k), \quad (8)$$

where

$$\phi_2(r_{ij}) = \varepsilon f_2\left(\frac{r_{ij}}{\sigma}\right), \quad (9)$$

$$\phi_3(r_{ij}) = \varepsilon f_3\left(\frac{r_{ij}}{\sigma}\right), \quad (10)$$

$$f_2(r) = \begin{cases} A(Br^{-p} - r^{-q})e^{\frac{1}{r-a}}, & r < a, \\ 0, & r > a, \end{cases} \quad (11)$$

$$f_3(i, j, k) = h(r_{ij}, r_{jk}, \theta_{ijk}) + h(r_{ji}, r_{ik}, \theta_{jik}) + h(r_{jk}, r_{ki}, \theta_{jki}), \quad (12)$$

$$h_{ijk}(r_{ij}, r_{jk}, \theta_{ijk}) = e^{\frac{\gamma}{r_{ij}^a} + \frac{\gamma}{r_{jk}^a}} \left( \cos \theta_{ijk} + \frac{1}{3} \right)^2. \quad (13)$$

$\varepsilon$  and  $\sigma$  are the energy and length units. The parameters  $p$  and  $q$  are usually taken to be 4 and 1, respectively,  $a$  represents the

cut-off distance to limit the atomic interactions in the range of the nearest-neighbor.  $\theta_{ijk}$  is the angle formed by the  $ij$  and  $jk$  bonds, which describes the direction nature of the covalent bond in the tetrahedral structure.  $\cos\theta_{ijk} = -\frac{1}{3}$  corresponds to the ideal structure.  $A$ ,  $B$  and  $\gamma$  are the bond strength parameters. The parameters of the SW empirical potentials for Ga-N and In-N are presented in Table 1 [7].

Table 1: Stillinger-Weber parameters for InN and GaN.

	Ga-N	In-N		Ga-N	In-N
$A$	7.7183	7.7546	$\lambda$	23.0425	15.3604
$B$	0.6937	0.6986	$\varepsilon(\text{eV})$	2.2645	1.9925
$a$	1.8	1.8	$\sigma(\text{\AA})$	1.7001	1.8790
$\gamma$	1.2	1.2			

These parameters give the good crystallographic parameters of the materials: the calculated bond lengths of Ga-N and In-N are 1.949Å and 2.156Å, respectively, similar to the experimental values. And the calculated elastic constants and bulk modulus seem in fair agreement with the experimental data [8]. The most stable structures obtained with these parameters are wurtzite and zinc-blende structures. These parameters are thus suitable to calculate the atomic configurations in InGaN alloys. In all of our calculation, the atomic structures were relaxed by using the Verlet algorithm. The periodic boundary conditions were used in the relaxation.

### 3.2. Case of InGaN alloys

We performed firstly a test of our SW potential in InGaN alloys. The random, ordering and cluster atomic configurations of Indium in InGaN alloy are considered. The stability of the alloys is described by the formation enthalpy of  $\text{In}_x\text{Ga}_{1-x}\text{N}$  with different In concentration

$$H = E_{\text{tot}} - xE_{\text{InN}} - (1-x)E_{\text{GaN}} \quad (14)$$

where  $E_{\text{InN}}$  and  $E_{\text{GaN}}$  are the energies of InN and GaN in their perfect structures.

For the case of the random distribution, the formation enthalpy is shown in Fig 2. The result is similar to that in ref. [9] except the narrow region around In=50%. Nevertheless, the formation enthalpy is positive in the whole range, which means the alloy is thermodynamically unstable. Especially for the high In concentration, there are InN clusters in the alloy. The distributions of bond length and atom energy of  $\text{In}_{0.5}\text{Ga}_{0.5}\text{N}$  are shown in Fig. 3 (a), (b). The results indicate that the bond length is mainly around the values of GaN(1.95 Å), InN(2.156Å), same to that in [10]. The deformation of the second- and high-order neighbors makes the distribution wide as a perturbation effect. The atom energy discretely distributes around -4.5eV, -4.35eV, -4.23eV, -4.05eV and -3.9eV, which corresponds to the different strain energies, i.e. five kinds of the nearest-neighbor atomic configurations. N atom is chosen as the center to analyze the atomic configuration and we find that the five energy values respectively correspond to N(4Ga), N(3Ga,1In), N(2Ga,2In), N(1Ga,3In) and N(4In).

### 3.3. Case of InGaN cluster in QW

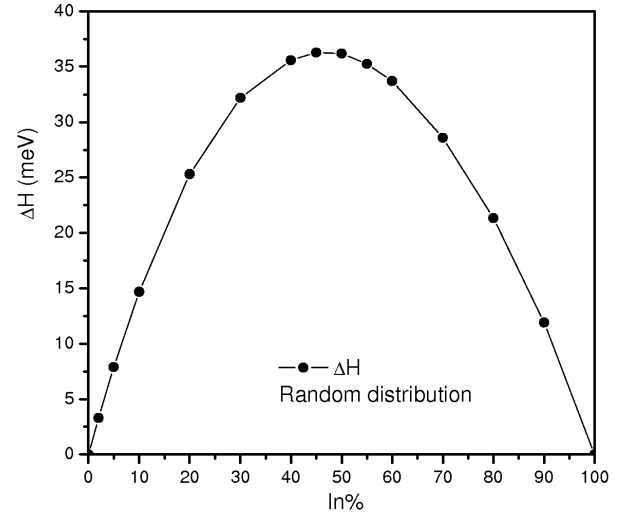


Figure 2: Formation enthalpy of  $\text{In}_x\text{Ga}_{1-x}\text{N}$  ( $0 < x < 1$ ).

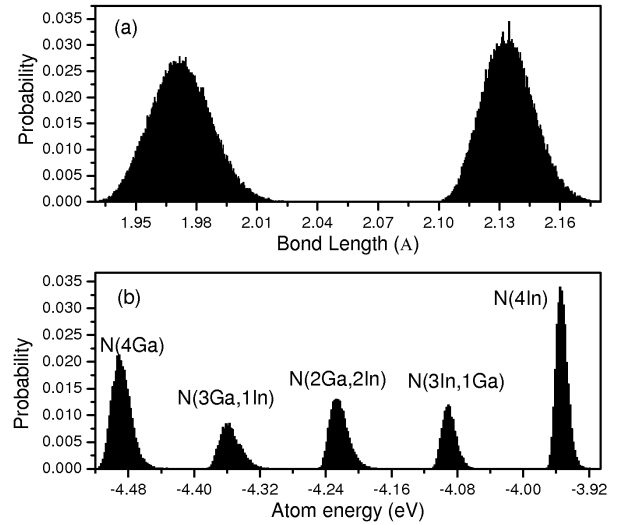


Figure 3: The distribution of bond length (a) and atom energy (b) in  $\text{In}_{0.5}\text{Ga}_{0.5}\text{N}$ .

In the centre of a set of 36 GaN monolayers stacked along the growth direction  $\langle 0001 \rangle$ , four monolayers (ML) of InGaN are embedded. The latter layers form a quantum well (QW), and the number of atoms is: 2868 N and 2868 (Ga, In). The average concentration in QW is 29.7% In at., or 977 In atoms. In the QW, one cluster is designed; its height along  $\langle 0001 \rangle$  is 10.42Å corresponding to the 4 monolayers of QW, and its length is 40Å in Fig. 4. Another 35Å large of cluster is considered also. Three In concentrations in the cluster were chosen as 10, 29.7 and 80% at, respectively. In the QW, Indium atoms are randomly distributed inside and outside of the cluster, no ordering is taken into account. It was previously shown that the formation enthalpy of a cluster is always higher than that of a QW without any cluster, except when the In concentrations in the cluster and outside are equal (29.7%).

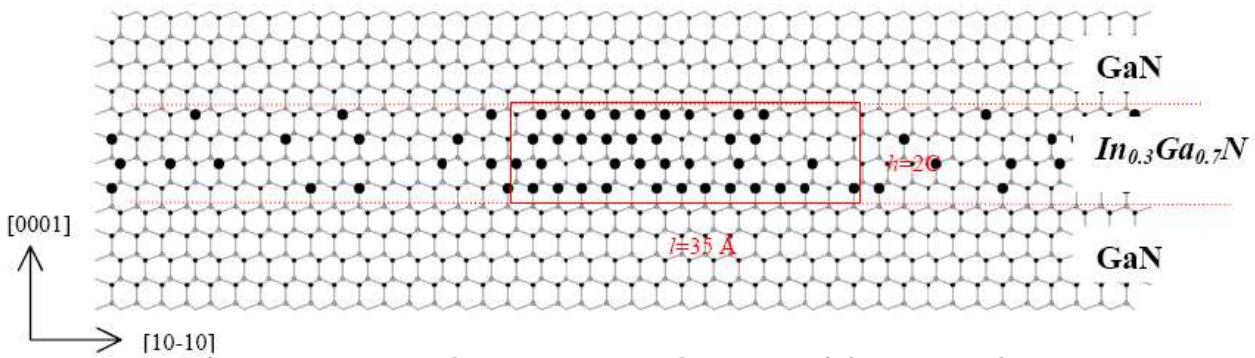


Figure 4: Calculation cell of a GaN/In<sub>x</sub>Ga<sub>1-x</sub>N/GaN heterostructure between two GaN layers containing an InN cluster.

A variation of the formation enthalpy is obtained as a function of the In concentration in the cluster, and we can note that the 29.65% In cluster shows the smallest energy whatever the size of the cell Fig. 5. This means that the homogeneous distribution of Indium atoms is more favourable than the formation of clusters in QW. No important difference was found in the bond angle distributions for the two cluster sizes with the same Indium concentration in the cluster. The angular distribution is shown in Fig. 6 for  $l=40\text{Å}$ . It is the smallest for the QW with 29.65% In. This angular deformation contributes to the largest energies in the cases of 10% and 80% Indium in the cluster.

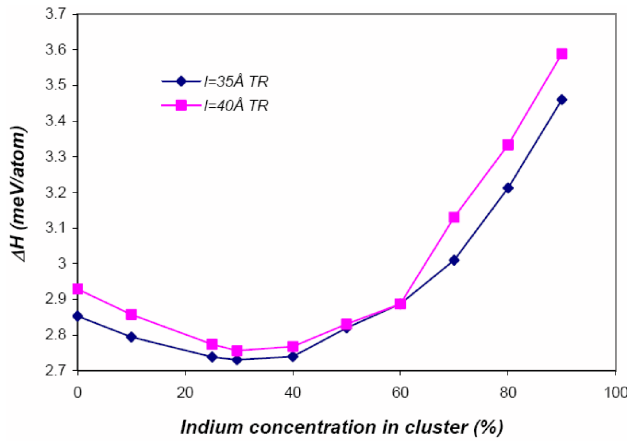


Figure 5: Formation enthalpy for two sizes of cluster, and for different concentrations of Indium in the cluster.  $l$  is the width of cluster, the length and height are the same.

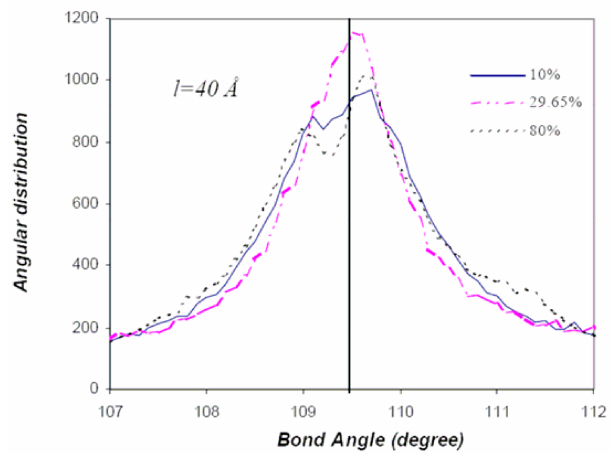


Figure 6: Angular distribution in QWs for  $l = 40\text{Å}$  with 10%, 29.65% and 80% In at. in the cluster. The centre line indicates the perfect angle of wurtzite crystal, equal to  $109.47^\circ$ .

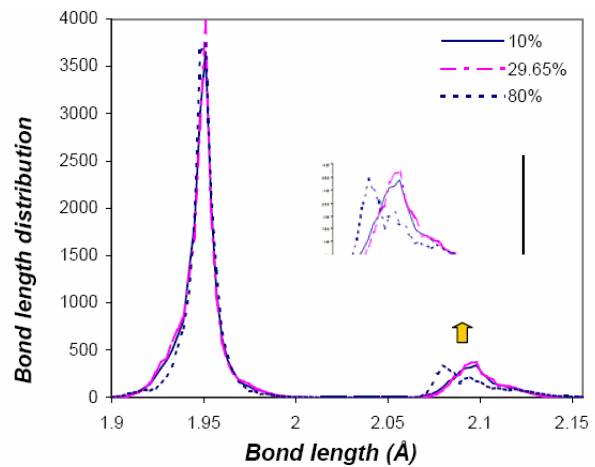


Figure 7: Bond length distribution in QWs,  $l=40\text{Å}$  for 10%; 29.65% and 80% In at.

Regarding the bond length distributions, the curves present the same shape for the two cluster sizes with the same Indium concentration. For the three different Indium concentrations, we can note that the peak is shifted slightly from the ideal GaN bond

length in the range 1.945Å to 1.951Å. In the case of 80% Indium, the shift is more pronounced (Fig. 7). As for the modification of the bond angle, the variation of the InN bonds lengths is an important contribution to the energy of the quantum well.

The calculation cell can be divided into three parts: (A) is the pure GaN, (B) and (C) are inside of the QW but (B) is outside of the cluster (C). In part (A), the GaN average bond length is found as 1.948Å whatever the In concentration in the QW.

The behaviours of a random alloy or of a cluster embedded in a matrix are quite different (Fig. 8). In both cases, the bonds remain distinct and the crystallographic rows are no more linear showing a significant fluctuation from the perfect lattice sites. Finally, the system relaxes in an intermediate state. However, for the embedded clusters, the QW structure of minimum energy depends also on the deformation rate of the host matrix. The atomic volume of InN is larger than that of GaN, and comparison of elastic constants shows that GaN is more rigid than InN. In these conditions, the expected equilibrium structure could be based on a slightly compressed GaN matrix, and a highly compressed InN cluster, these effects being controlled by the In concentration in the cluster.

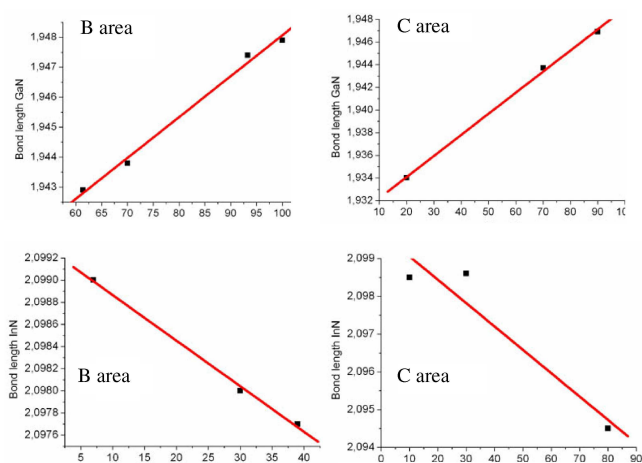


Figure 8: Variation of the GaN and InN bond lengths[Å] in (B) outside of the cluster and in (C) inside of the cluster.

#### 4. Conclusion

In the first part of our calculations we have shown that the residual stresses induced by threading dislocations are too small driving forces to form quantum dots (QDs) with Indium concentrations greater than 70-80%. In other words the residual stresses induced TD can be treated as the dominant driving force which can nucleate QDs but to form a QD with concentration higher than 70-80%  $\frac{\text{In}}{\text{Ga+In}}$  fraction an additional driving force must be taken into account. As it is easy to guess this additional driving force responsible for Indium segregation over 80% can be the osmotic force induced by a pure chemical part of chemical potential  $\frac{\partial \psi_{\text{ch}}}{\partial x}$  which was neglected in the present calculations. Summing up, we have demonstrated how far the segregation of Indium in InGaN layer can be interpreted in terms of residual stresses induced by threading dislocation.

In the second part by using a Stillinger-Weber potential, we have analysed the InGaN quantum wells with a fixed Indium rate

29.65%. The formation of clusters with different Indium concentrations was considered, and this formation is not supported in this approach since the homogenous distribution of In atoms leads to a lowest formation enthalpy. However, in some cases the difference in energy is very low, and a metastable formation of clusters could be expected.

#### 5. Acknowledgement

This work is supported by EU Marie Curie RTN contract MRTN-CT-2004-005583 (PARSEM) and grant 131/6PRUE/2005/7 founded by the Polish Ministry of Science and Higher Education.

#### References

- [1] Stephenson, G.B., Deformation during interdiffusion, *Acta metall.* **36**, 2663 (1988).
- [2] Wu, Ch.H., The role of Eshelby stress in composition-generated and stress assisted diffusion, *J. Mech. Phys. Solids* **49**, 1771 (2001).
- [3] Dłużewski, P., Nonlinear field theory of stress induced diffusion, *Defect and Diffusion Forum* **237-240**, 107 (2005).
- [4] Dłużewski, P., Jurczak, G., Maciejewski, G., Kret, S., Ruterana, P. and Nouet, G., Finite element simulation of residual stresses in epitaxial layers, *Mater. Sci. Forum* **404-405**, 141 (2002).
- [5] Aïchoune, N., Potin, V., Ruterana, P., Hairie, A., Nouet, G. and Paumier, E., An empirical potential for the calculation of the atomic structure of extended defects in wurtzite GaN, *Comput. Mater. Sci.* **17**, 80 (2000).
- [6] Ruterana, P., Singh, P., Kret, S., Jurczak, G., Maciejewski, G., Dłużewski, P., Cho, H.K., Choi, R.J., Lee, H.J., and Suh, E.K., Quantitative evolution of the atomic structure of defects and composition fluctuations at the nanometer scale inside InGaN/GaN heterostructures, *phys. stat. sol. (b)* **241** (2004) 2735.
- [7] Lei, H.P., Chen, J., Petit, S., Ruterana, P., Jiang, X.Y., Nouet, G., Stillinger-Weber parameters for In and N atoms, *Superlattices and Microstructures* **40** (2006).
- [8] Levinshtein, M.E., Rumyantsev, S.L. and Shur, M.S., *Properties of Advanced Semiconductor Materials*, John-Wiley & Sons, (2001).
- [9] Grosse F. and Neugebauer, J., Limits and accuracy of valence force field models for  $\text{In}_x\text{Ga}_{1-x}\text{N}$  alloys, *Phys. Rev. B* **63**, 085207 (2001).
- [10] Saito, T., Arakawa, Y., Atomic structure and phase stability of  $\text{In}_x\text{Ga}_{1-x}\text{N}$  random alloys calculated using a valence-force-field method, *Phys. Rev. B* **60**, 1701 (1999)
- [11] Dłużewski, P., Nonlinear field theory of the stress induced interdiffusion and mass transport, accepted for publication in *Defect and Diffusion Forum* (2006).